Optimizing Power Density and Efficiency of a Double-Halbach Array Permanent-Magnet Ironless Axial-Flux Motor

Kirsten P. Duffy – University of Toledo / NASA GRC

Background

Hybrid Electric and Turboelectric Aircraft Propulsion

Boeing SUGAR

NASA STARC-ABL

NASA N3X

Background

Turboelectric Propulsion Benefits

Electric drive = motor + generator + other electrical components

Break-Even on Weight

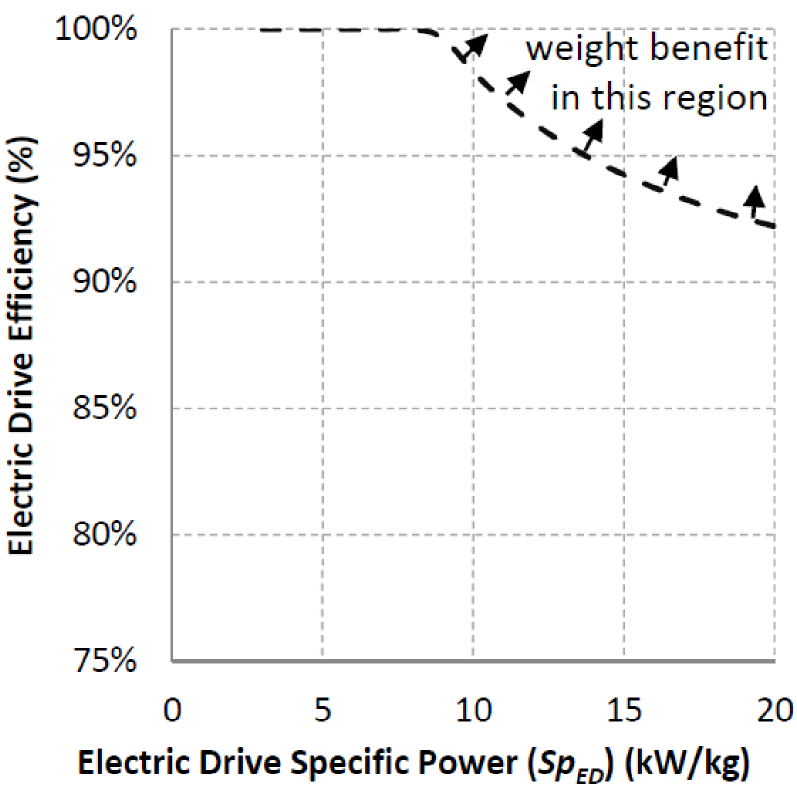

Each aircraft configuration will yield combinations of power density and efficiency required to achieve net benefit

From Jansen et al. "Turboelectric Aircraft Drive Key Performance Parameters and Functional Requirements"

Target Application

- Example – HEIST (Hybrid-Electric Integrated Systems Testbed)
- 31-foot span wing section
- 18 fans directly driven by electric motors
- Motors powered by batteries
- Motor dimensions: 5.5” diameter, 2” length
- Target: 13 kW power at 7200 RPM

➢ *Our motor design: target 13 kW/kg and 1% loss*

http://climate.nasa.gov/news/2286/leaptech-demonstrates-electric-propulsion-technologies/

Analysis

Double-Halbach PM Array
Ironless Axial Flux Motor

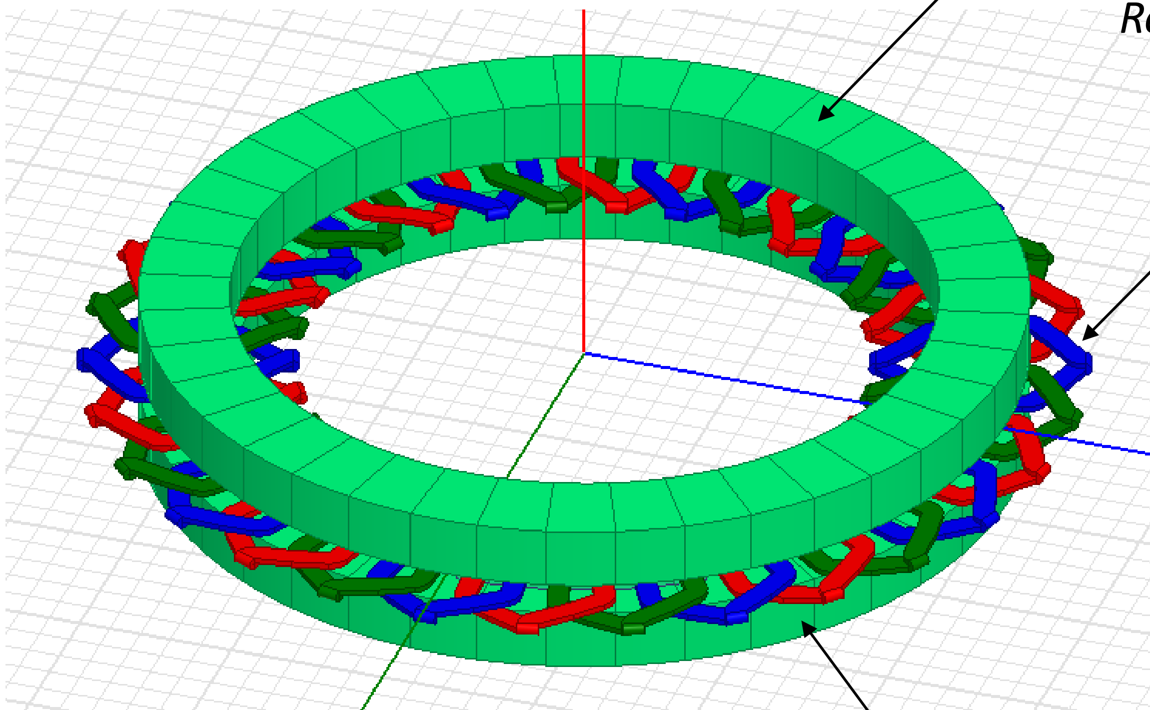

Analysis

Double-Halbach PM Array Ironless Axial Flux Motor

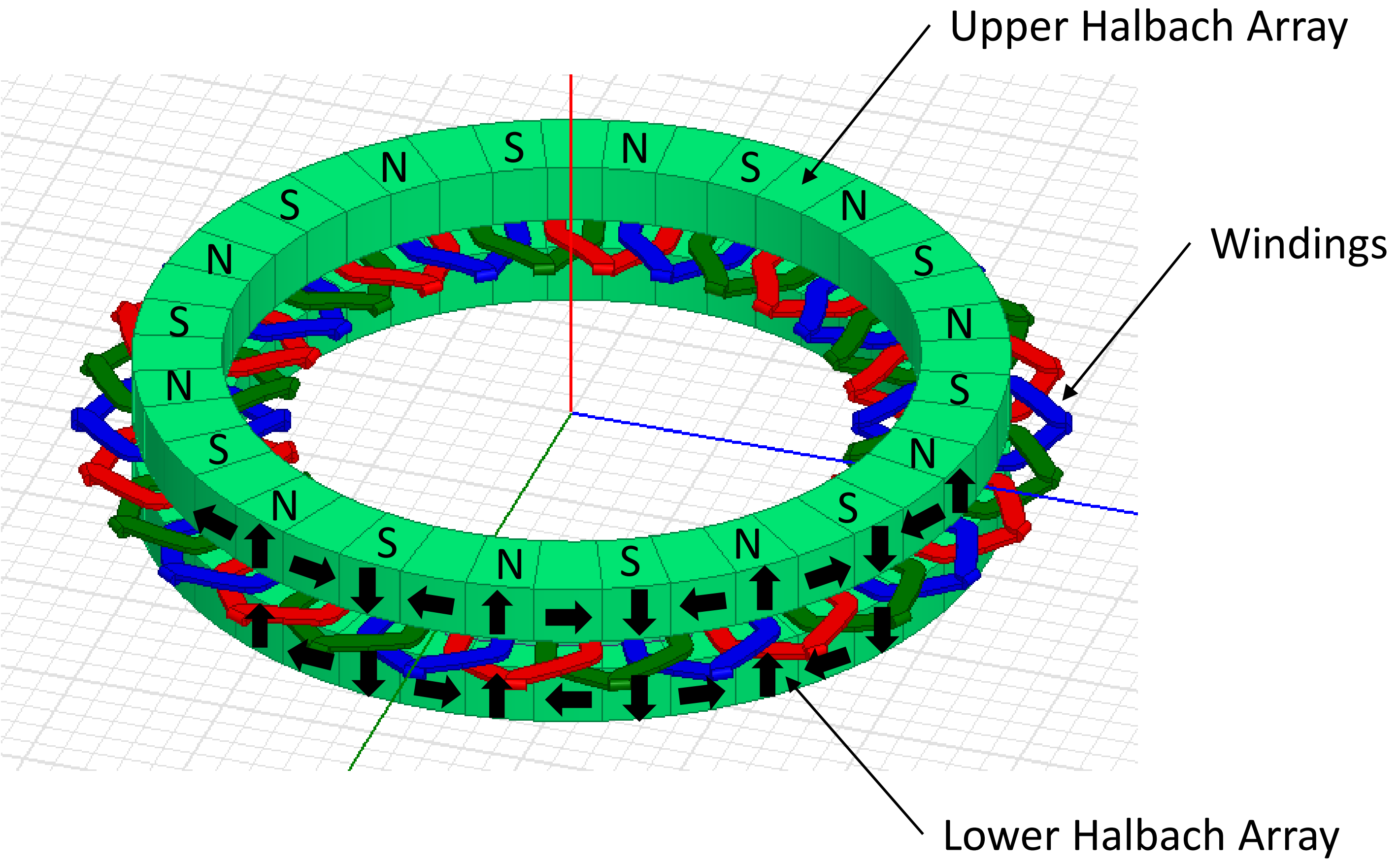

Analysis

Double-Halbach PM Array
Ironless Axial Flux Motor

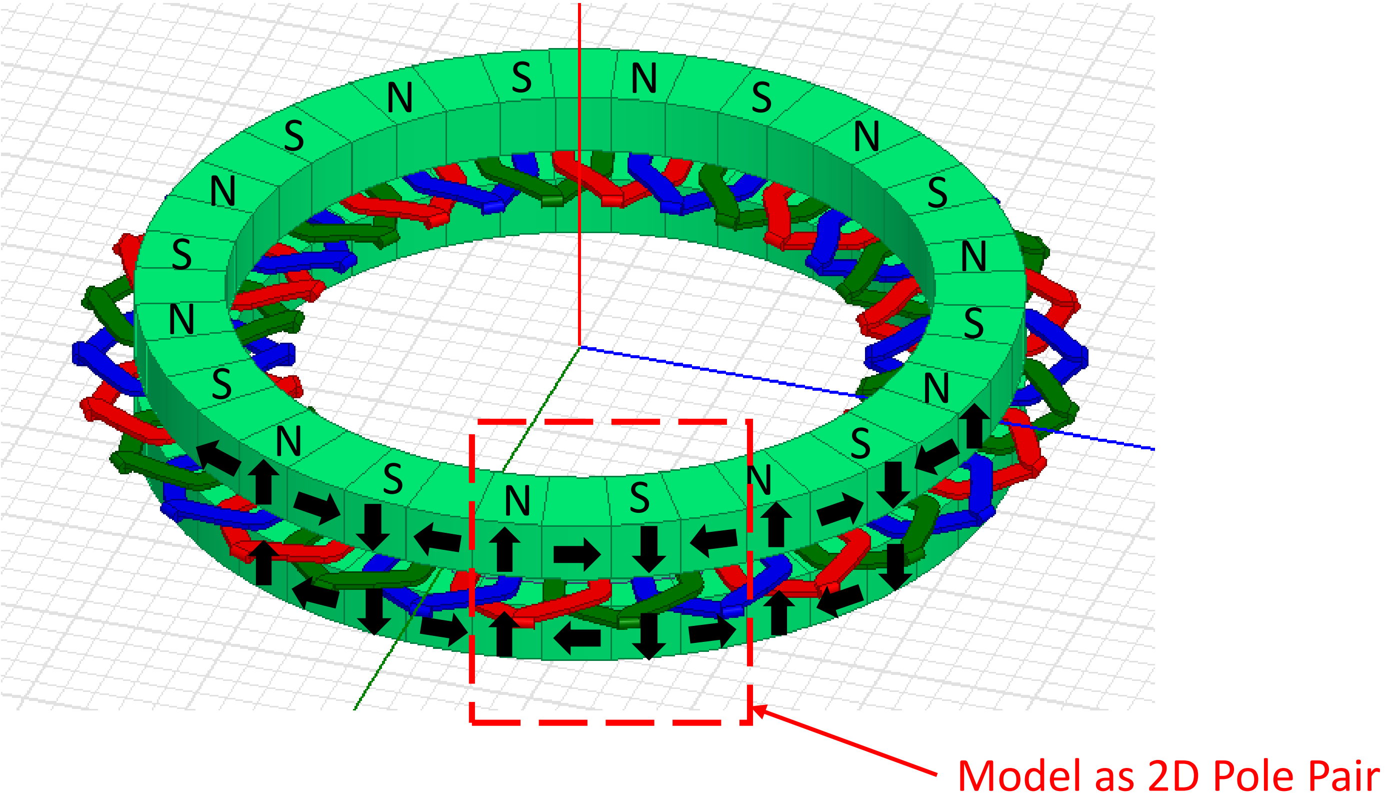

Analysis

Pole Pair Analysis

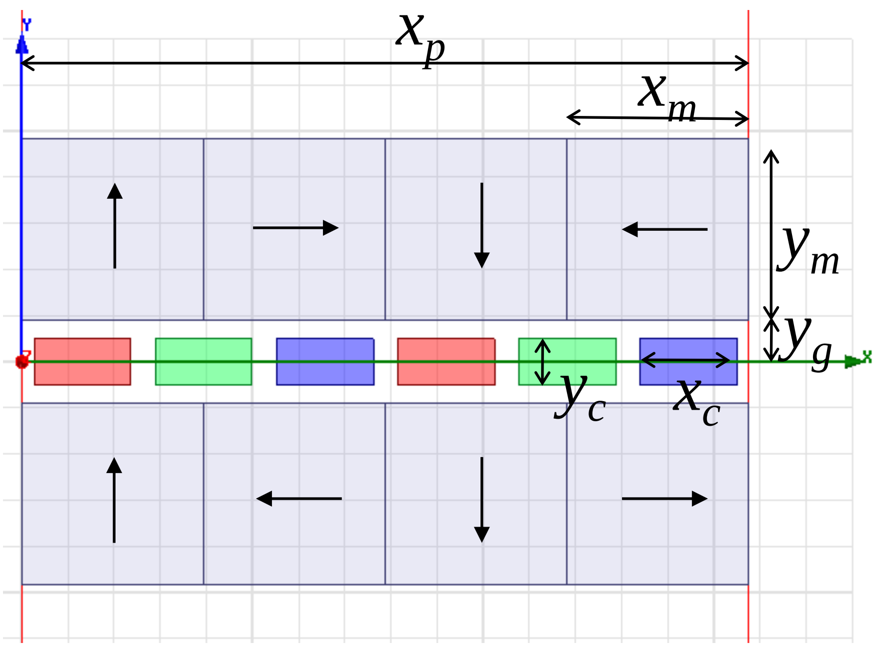

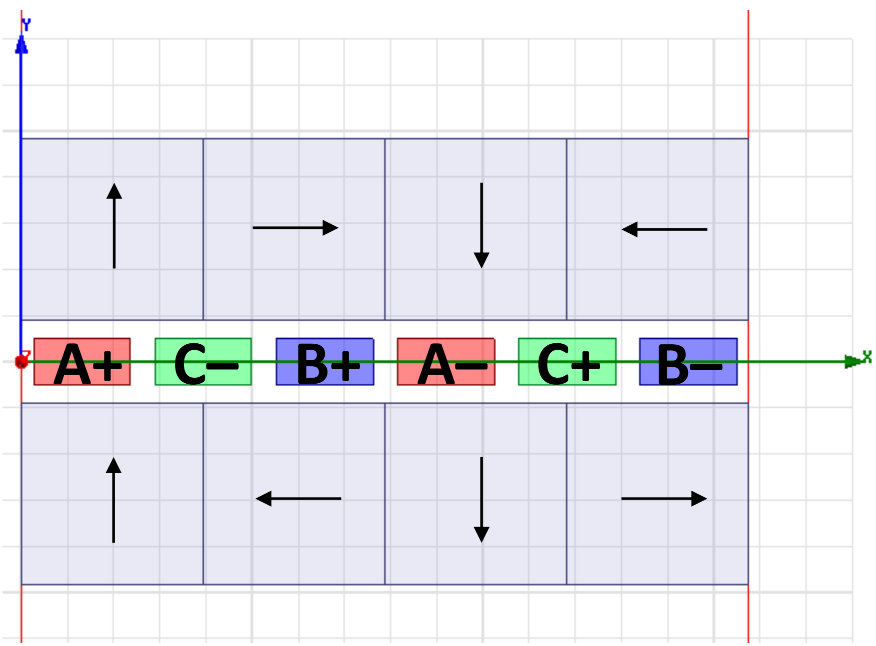

2D magnetostatic pole pair model allows for simple equation-based analysis

Analysis

Pole Pair Analysis

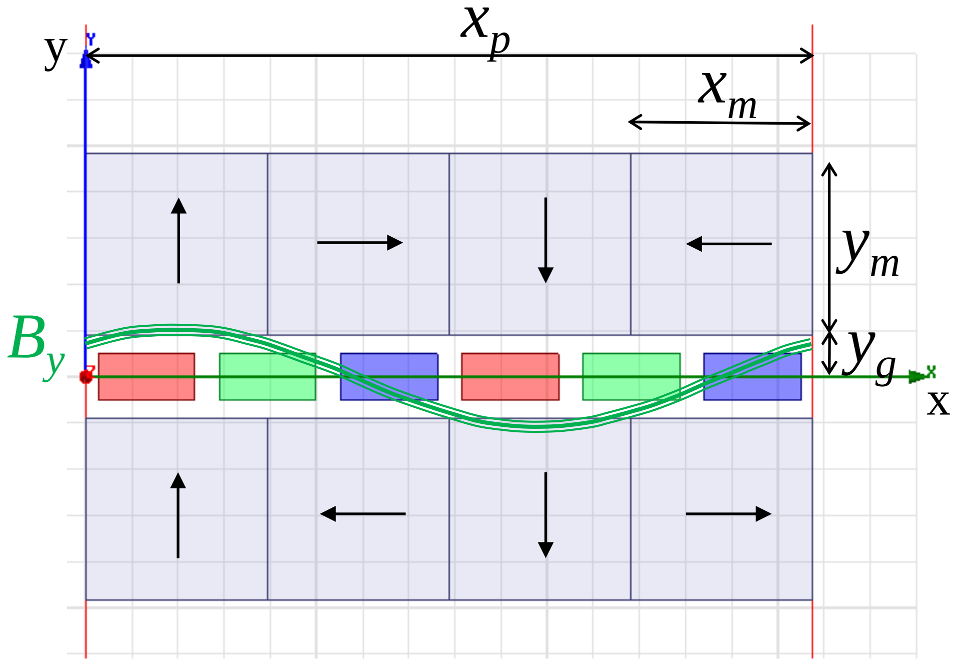

$$B_y = 2B_R e^{-ky_g}\left(1 - e^{-ky_m}\right)\frac{\sin(\epsilon\pi/n_m)}{\pi/n_m}\cos kx \cosh ky$$

$$F_c = J\Delta r \int_{x_1}^{x_2}\int_{y_1}^{y_2} B_y \, dxdy$$

$k = 2\pi/x_p$

Analysis

Pole Pair Analysis

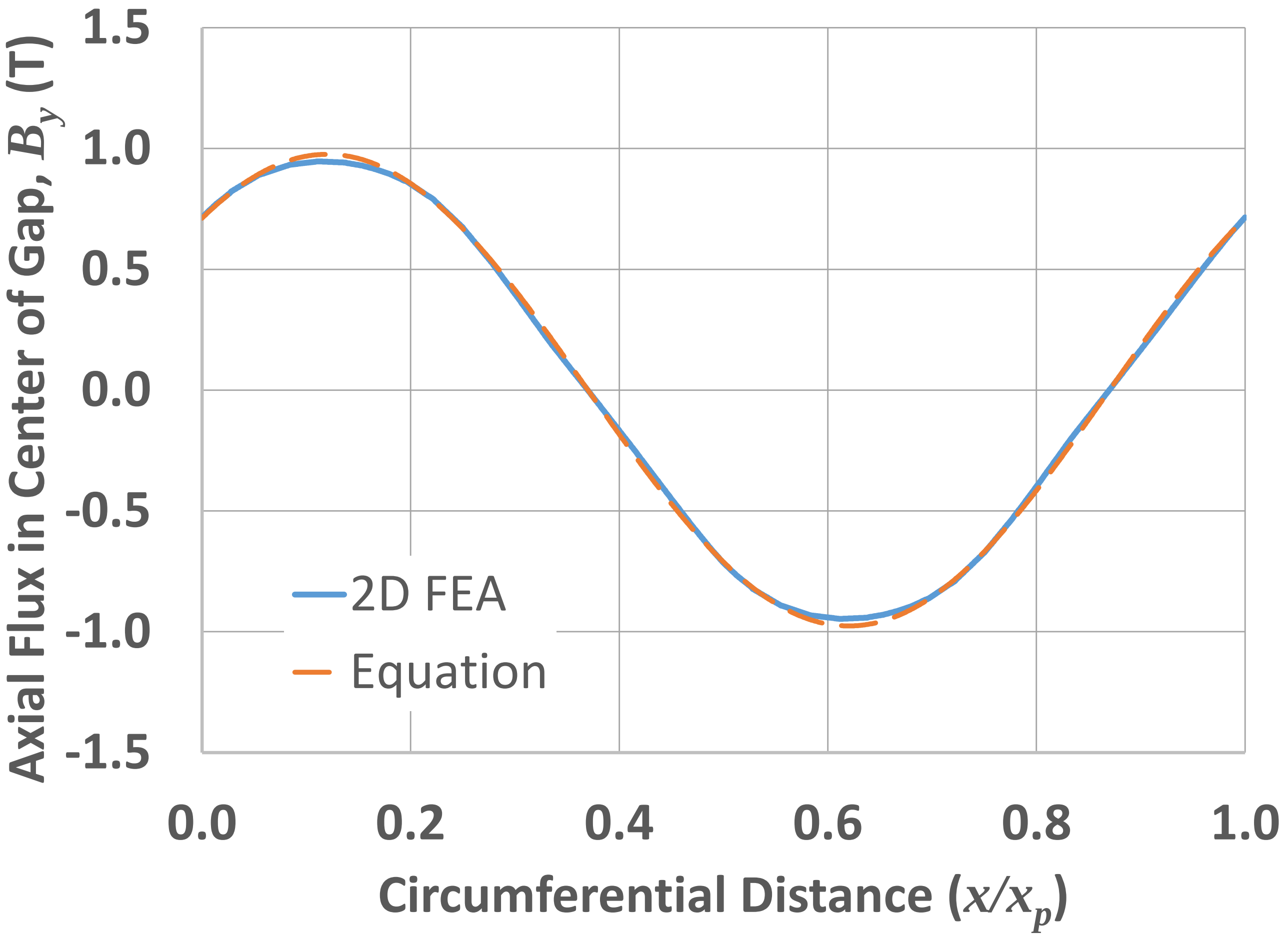

Analysis

Force/Torque/Power

$$F_c = \left[2JB_R\Delta r y_g y_m\right]\left[\frac{e^{-ky_g}}{ky_g}\right]\left[\frac{1-e^{-ky_m}}{ky_m}\right]\left[\frac{\sin(\epsilon\pi/n_m)}{\pi/n_m}\right]\sin kx\Big|_{x_1}^{x_2}\sinh ky\Big|_{y_1}^{y_2}$$

$$F_p = \sum_{c=1}^{6} F_c \qquad T = pr_aF_p \qquad P = T\,\omega_r = T\,RPM\;\pi/30$$

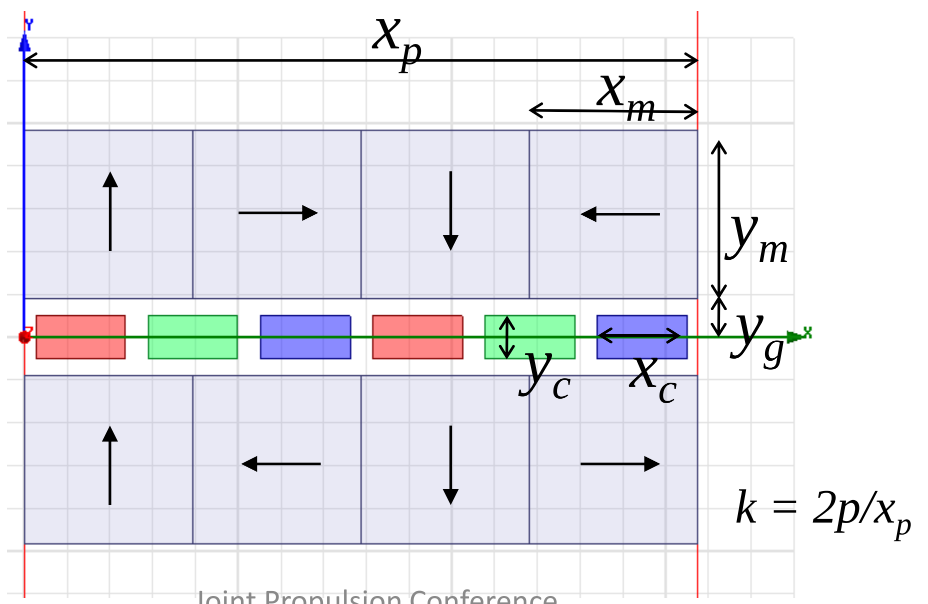

Analysis

Power Density – Based on Magnet Mass

$$\frac{P}{m_m} \propto \left[\frac{J B_R v_{tip}}{\rho_m}\right]\left[e^{-k y_g}\right]\left[\frac{1-e^{-k y_m}}{k y_m}\right]\left[\frac{\sin(\epsilon\pi/n_m)}{\pi/n_m}\right]$$

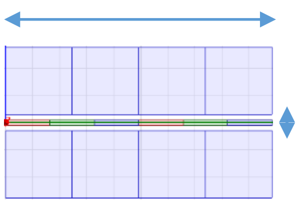

Small gap / pole size
high power density

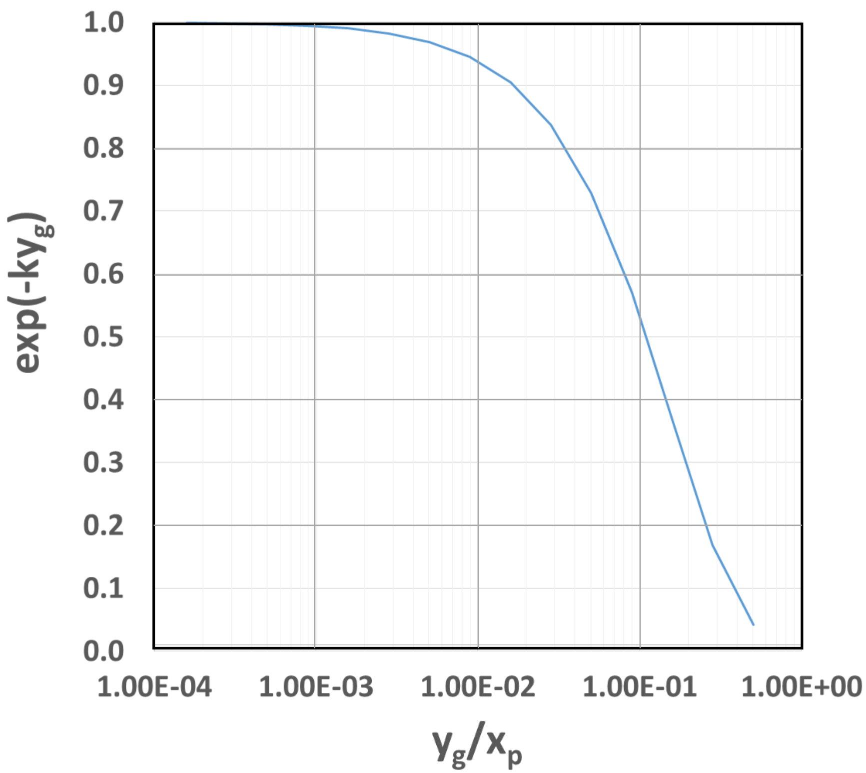

Ratio of gap to pole size

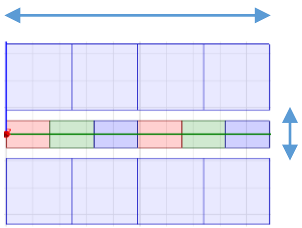

Large gap / pole size
low power density

Analysis

Power Density – Based on Magnet Mass

$$\frac{P}{m_m} \propto \left[\frac{JB_R v_{tip}}{\rho_m}\right]\left[e^{-ky_g}\right]\left[\frac{1-e^{-ky_m}}{ky_m}\right]\left[\frac{\sin(\epsilon\pi/n_m)}{\pi/n_m}\right]$$

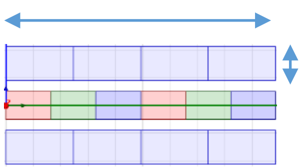

Small magnet thickness to pole size high power density

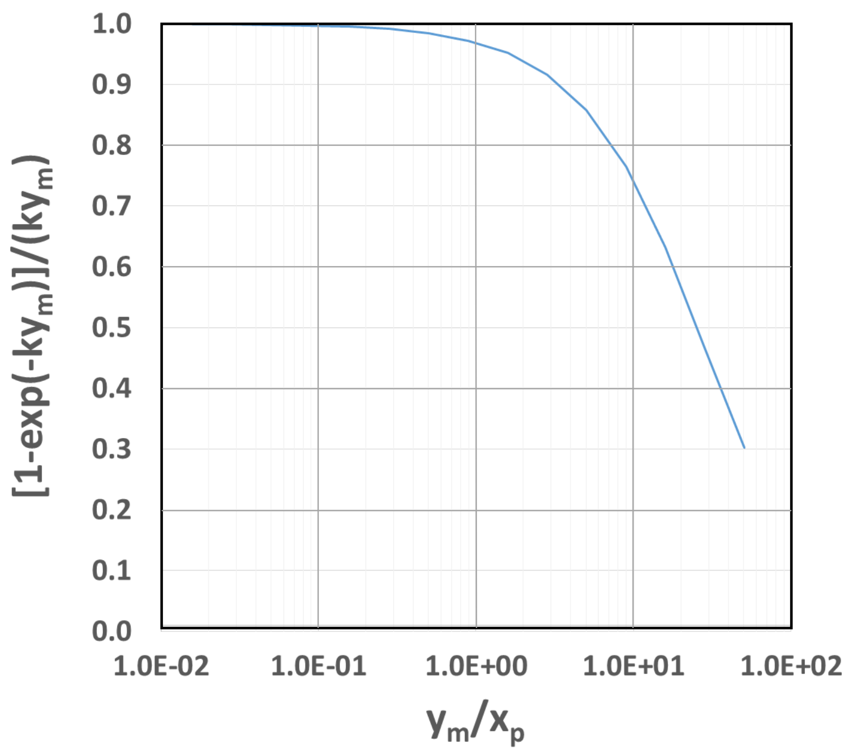

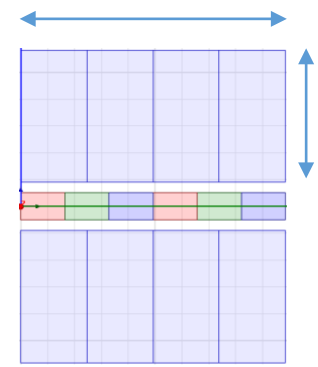

.arge magnet thickness to pole size low power density

Ratio of magnet thickness to pole size

Analysis

Power Density – Based on Magnet Mass

$$\frac{P}{m_m} \propto \left[\frac{JB_R v_{tip}}{\rho_m}\right]\left[e^{-ky_g}\right]\left[\frac{1-e^{-ky_m}}{ky_m}\right]\left[\frac{\sin(\epsilon\pi/n_m)}{\pi/n_m}\right]$$

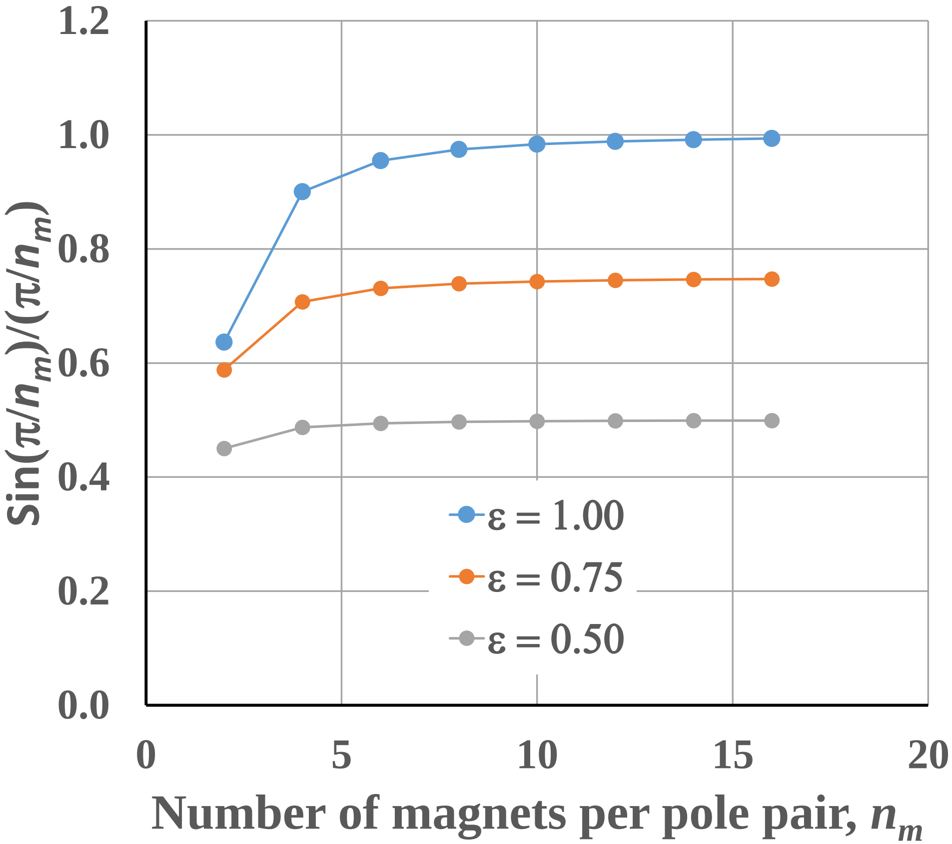

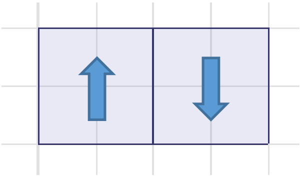

ε = 1, n_m = 2

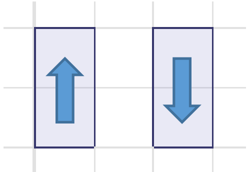

ε = 0.5, n_m = 2

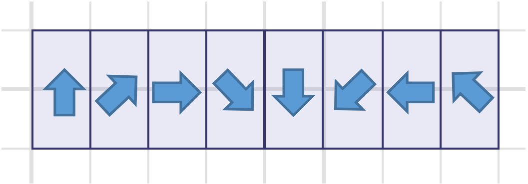

ε = 1, n_m = 8

Analysis

Parameter	Value
Target power	13 kW
Target power density	13 kW/kg Based on magnet and winding mass only
Target loss	< 1% Including magnet and winding losses only
Outer diameter	5.5 inches (140 mm)
Magnet remanence flux, B_R	1.4 T (NdFeB)
Current density, J	3 A/mm^2 (natural convection) to 30 A/mm^2 (liquid cooling)
Electrical frequency, f	< 2000 Hz ≤ 16 pole pairs at 7200 RPM

Results

Power

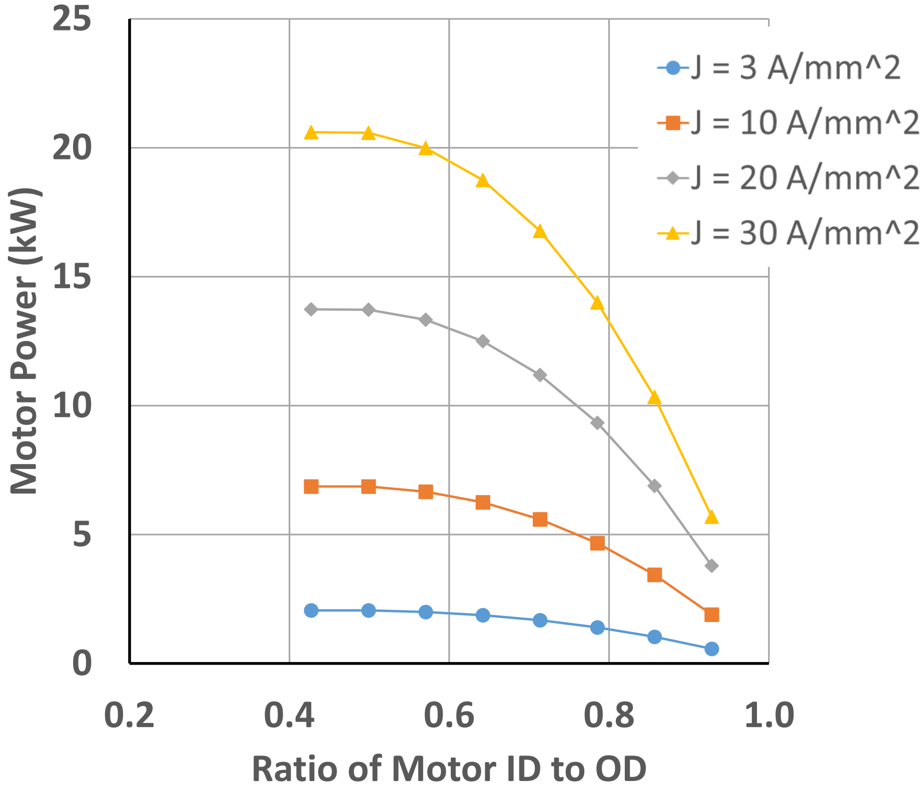

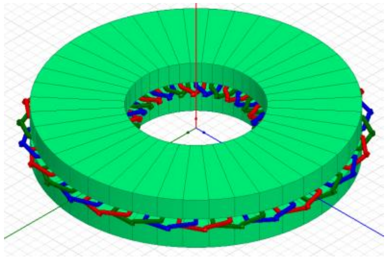

Low ID/OD

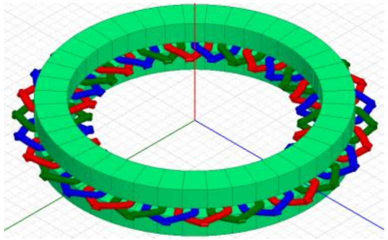

High ID/OD

y_c = 3 mm, 16 pole pairs, magnet aspect ratio y_m/x_m = 1

16 pole pairs → f = 1920 Hz

Results

Power Density

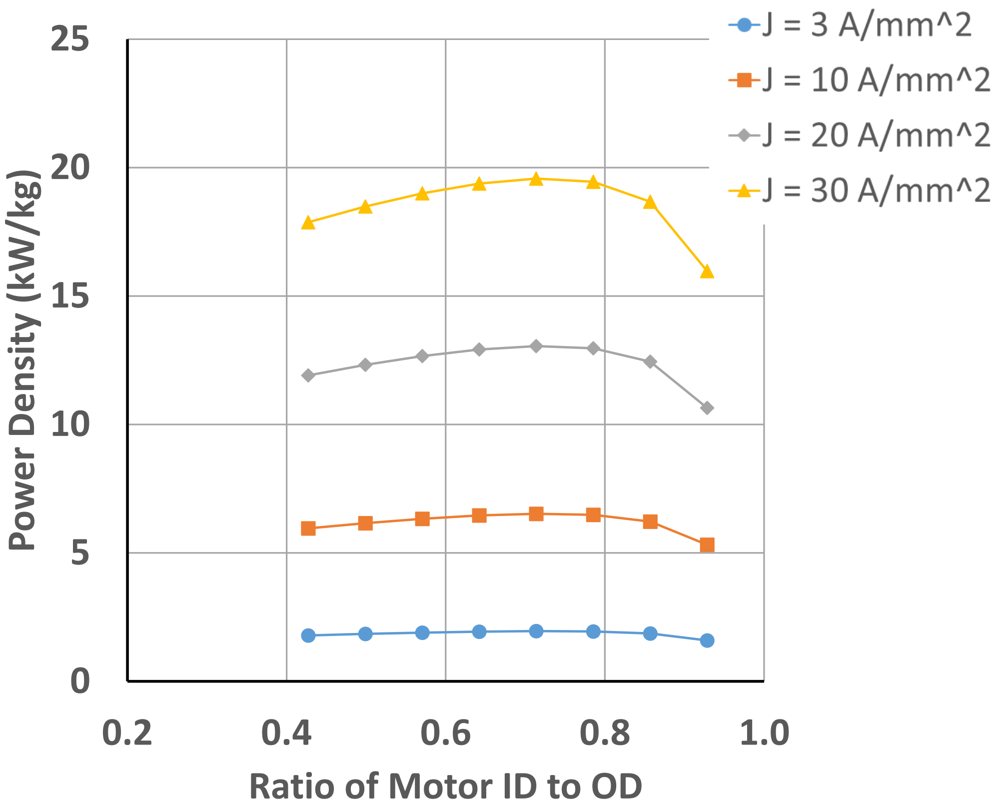

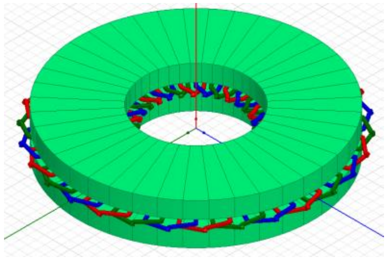

Low ID/OD

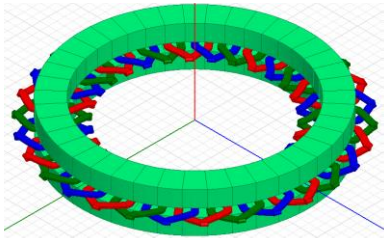

High ID/OD

y_c = 3 mm, 16 pole pairs, magnet aspect ratio y_m/x_m = 1

16 pole pairs → f = 1920 Hz

Results

I²R Loss P_c $\qquad P_c \propto \frac{J_{rms}^2 V_c}{\sigma \eta}$

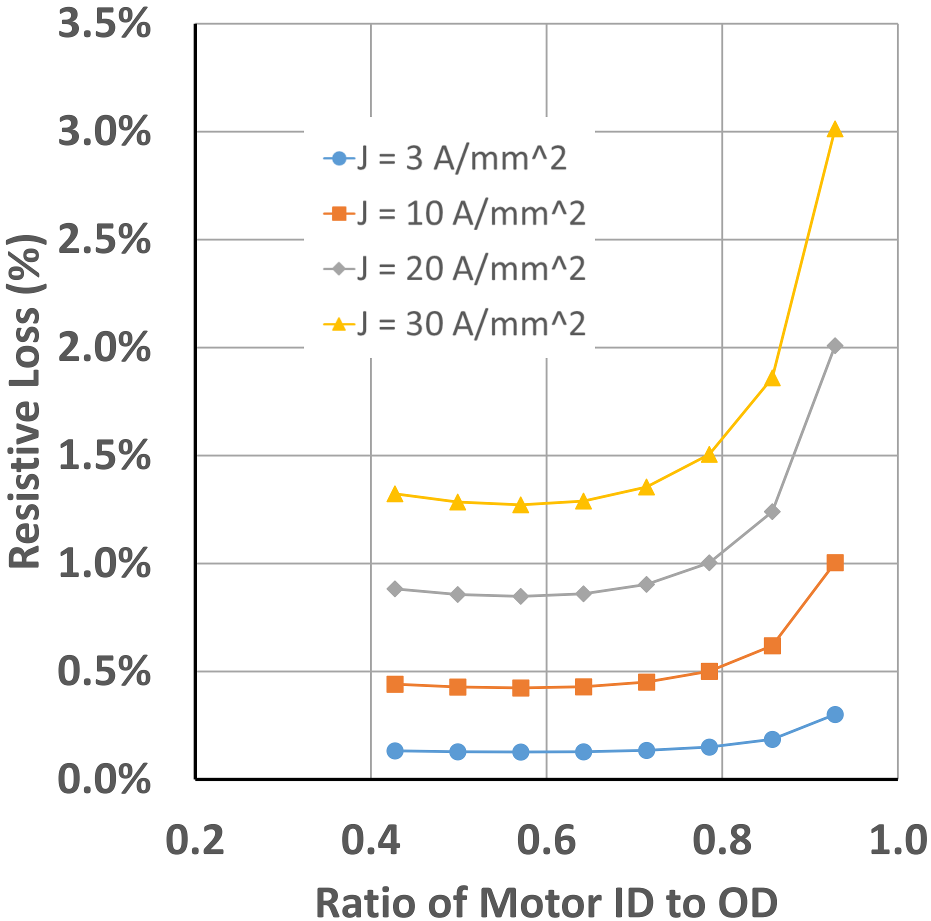

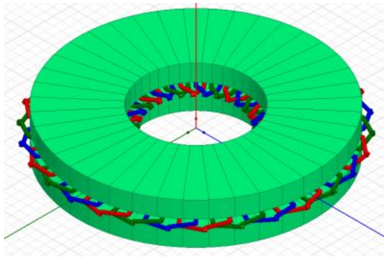

Low ID/OD

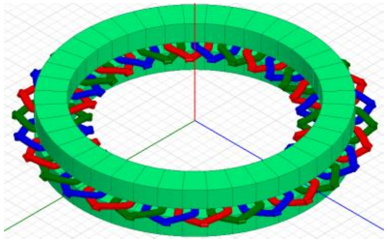

High ID/OD

Results

Conductor Eddy Loss P_e

$$P_e \propto \sigma f^2 d^2 B_{pk}^2 V_c$$

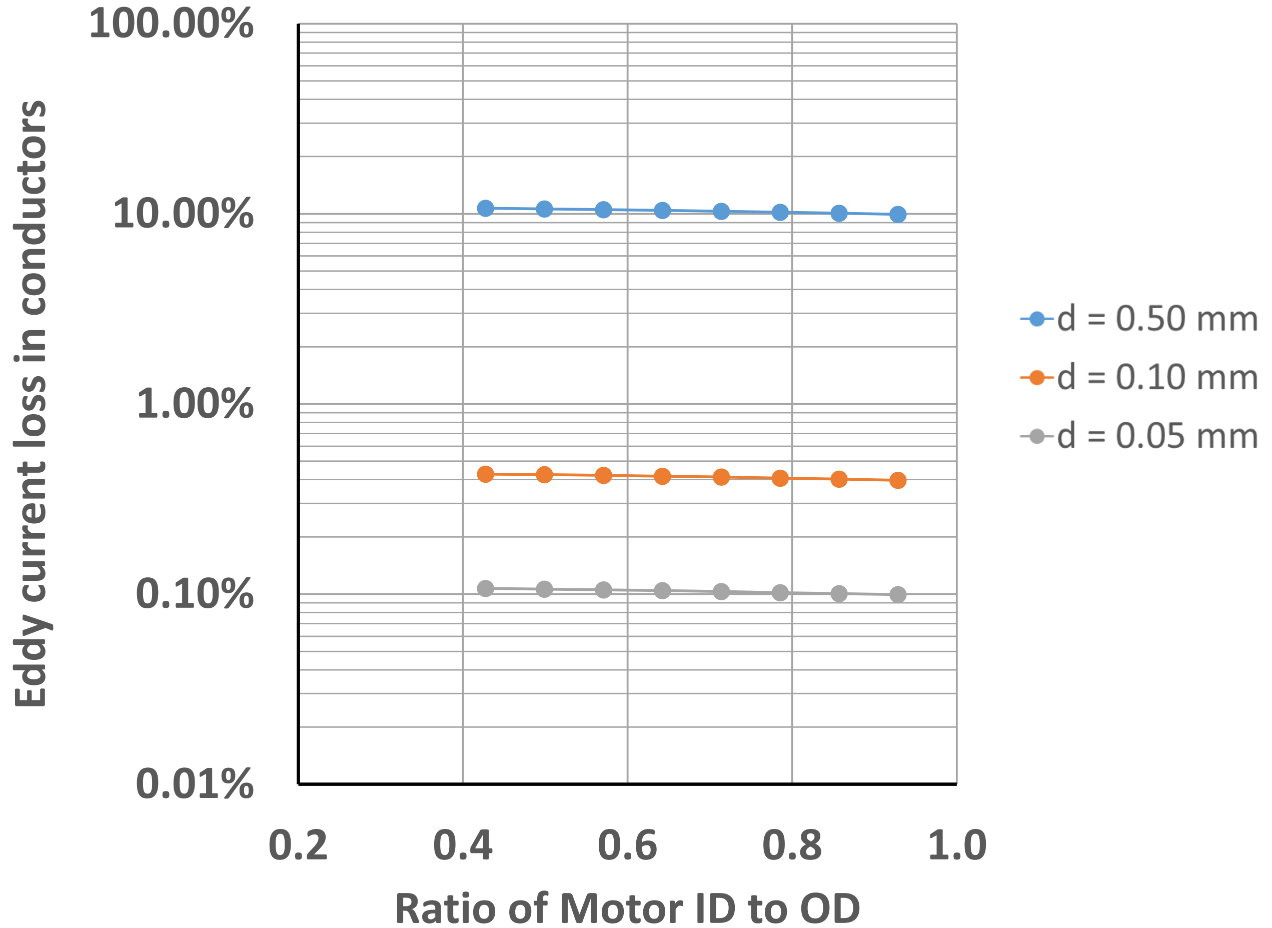

Results

Effect of Magnet Aspect Ratio

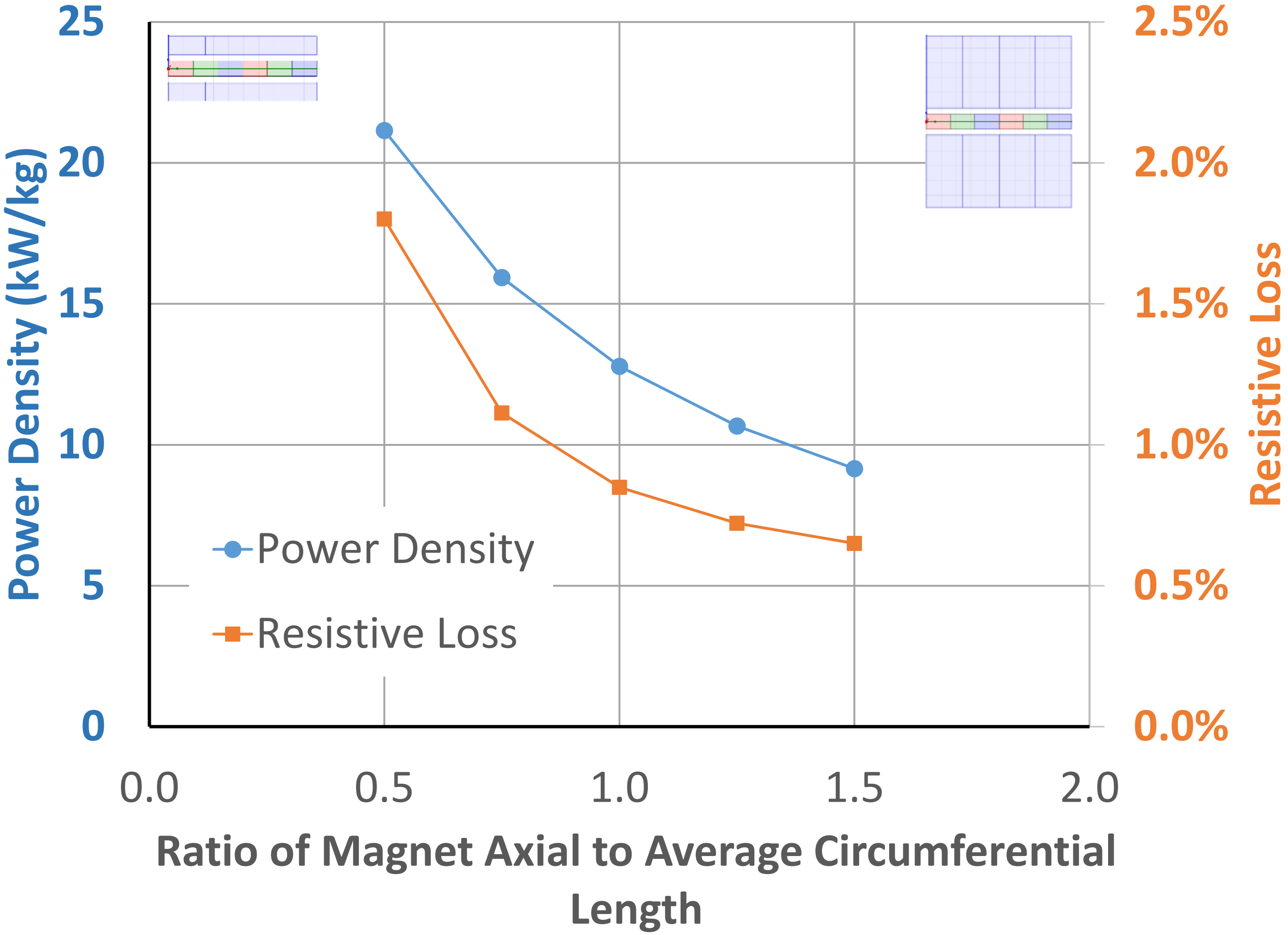

Rotor ID/OD = 0.6, y_c = 3 mm, 16 pole pairs

Results

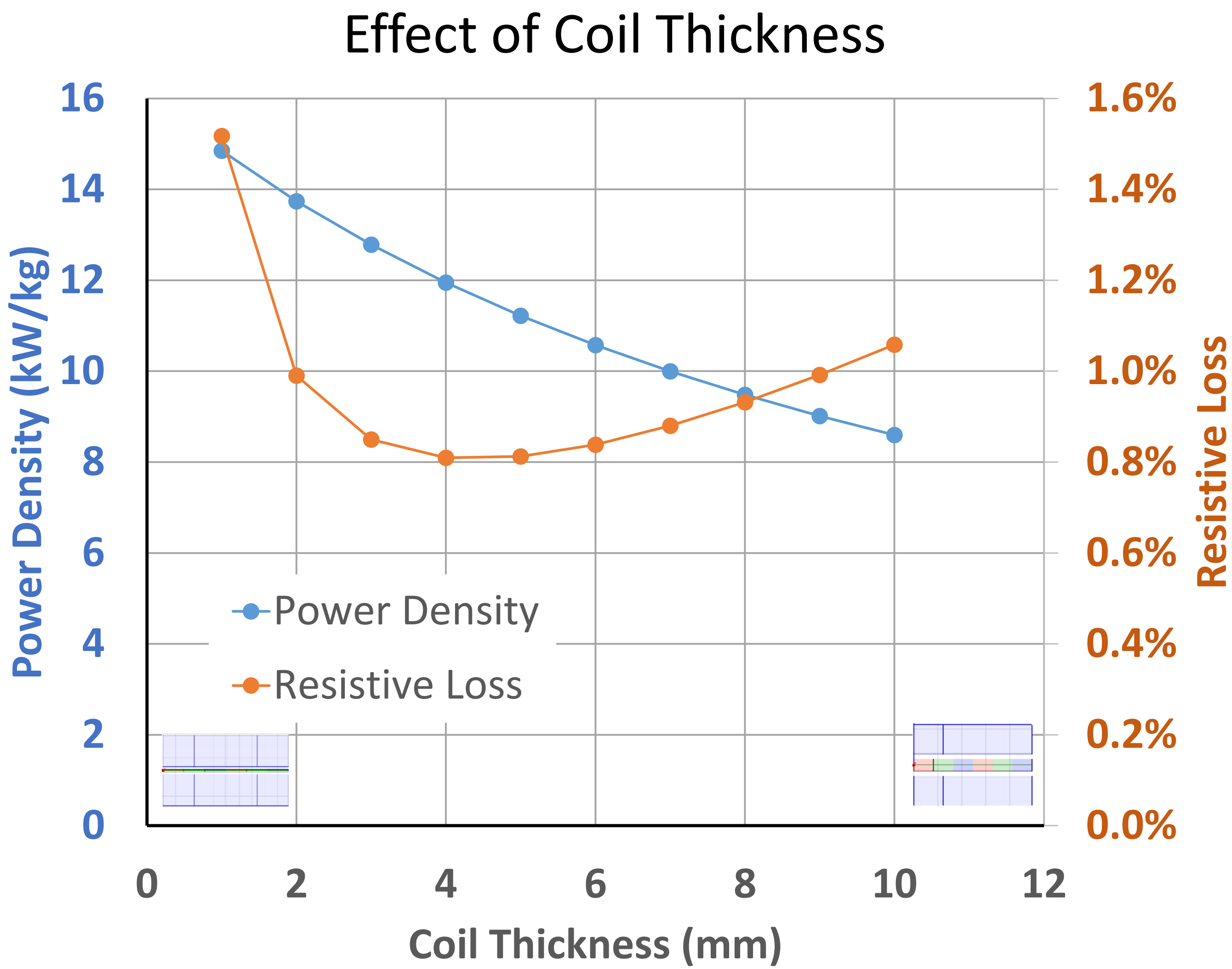

Rotor ID/OD = 0.6, y_c = 3 mm, 16 pole pairs

Results

Effect of Number of Pole Pairs

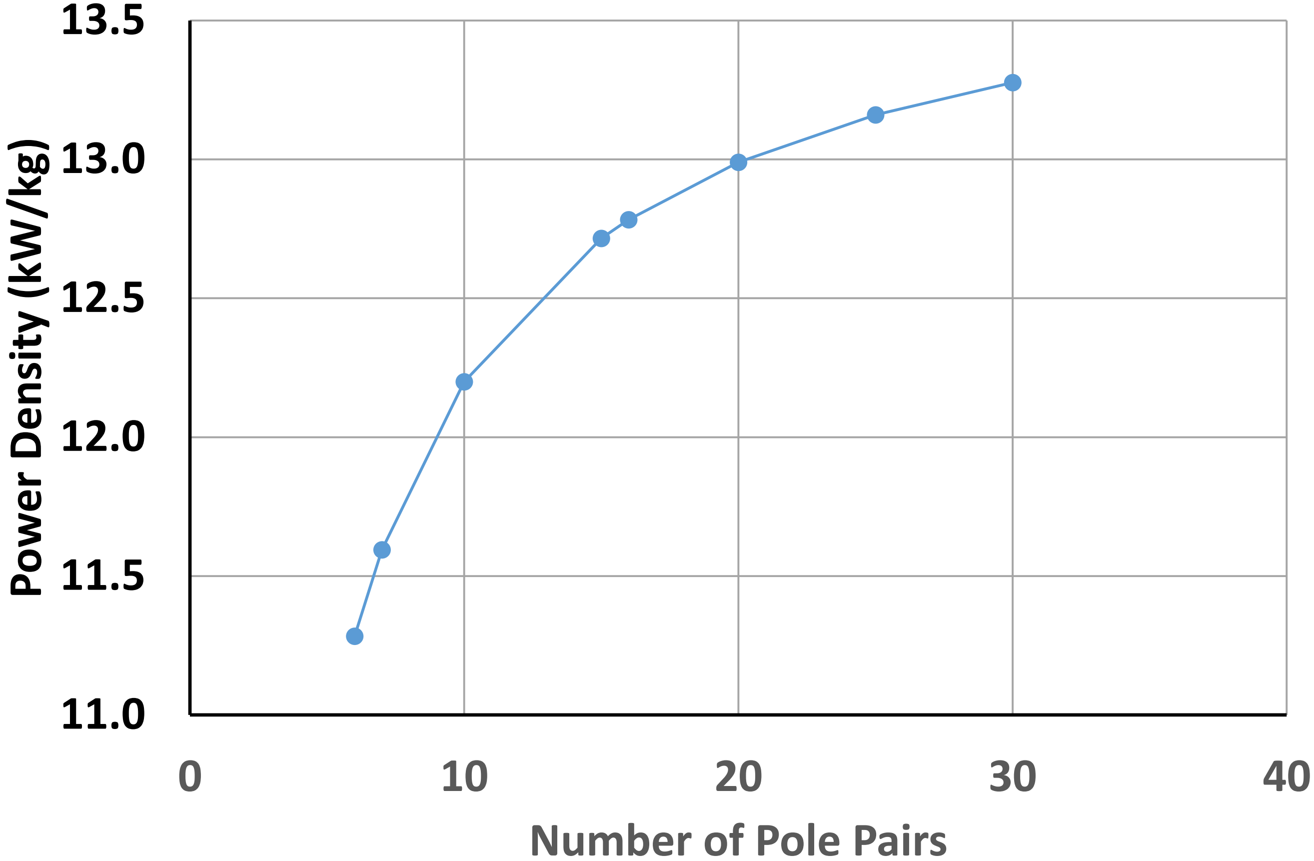

B_{max} = 1.0 T

Results

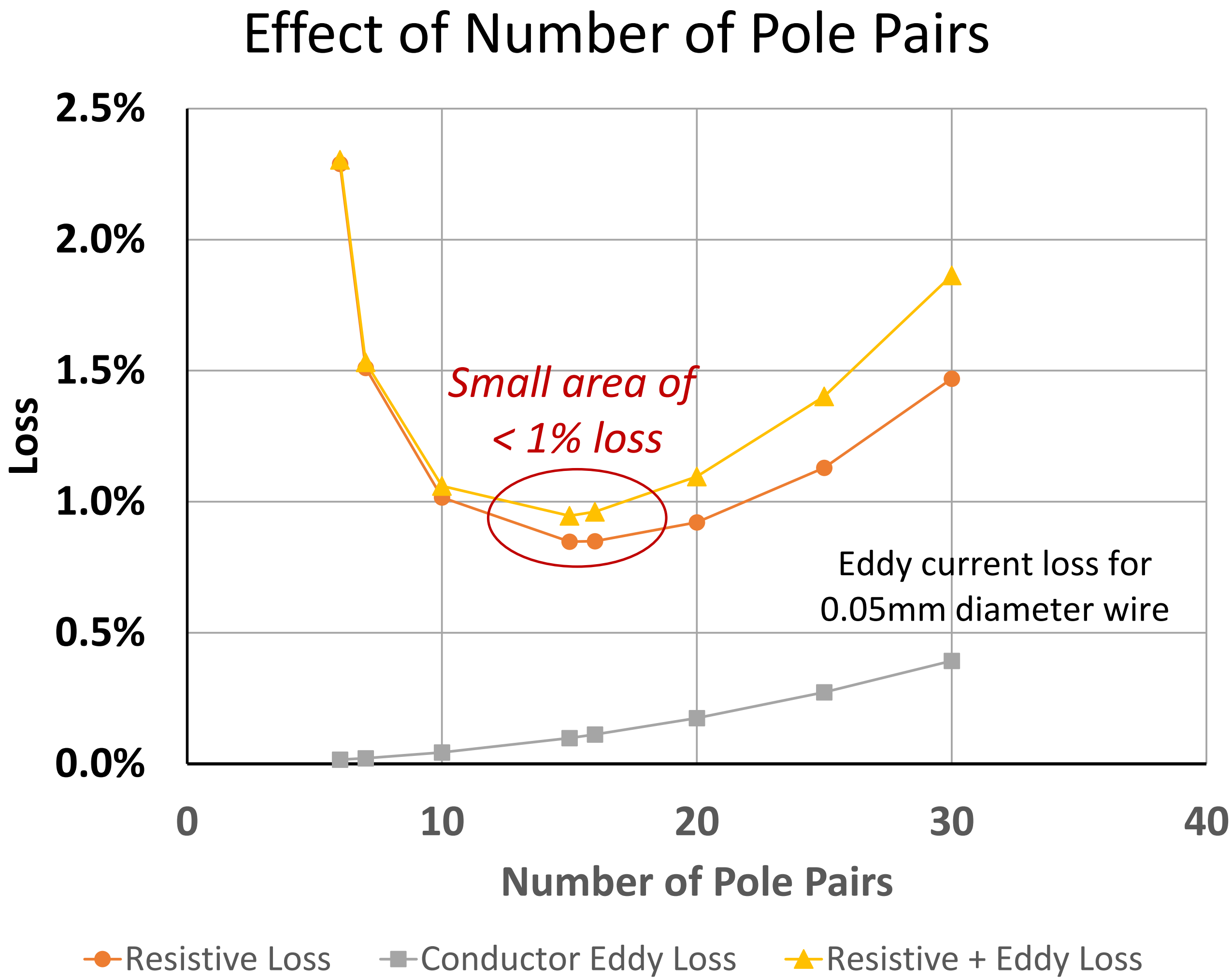

B_{max} = 1.0 T

Results

Final Motor Performance

Verified with Maxwell 3D FEA

Parameter	Value
Power	13 kW at 7200 RPM
Power density	12.8 kW/kg Based on magnet and winding mass only
Loss	0.85% - conductor resistive loss 0.11% - conductor eddy current loss 0.02% - magnet eddy current loss (3D FEA)
ID/OD = 0.6, Coil thickness = 3 mm, 16 pole pairs, 20 A/mm^2 current density, and magnet aspect ratio = 1	

- *Difficult to achieve goal of 13 kW/kg and 1% loss in this configuration*
- *Required 20 A/mm^2 which will require cooling*

Conclusions/Future Work

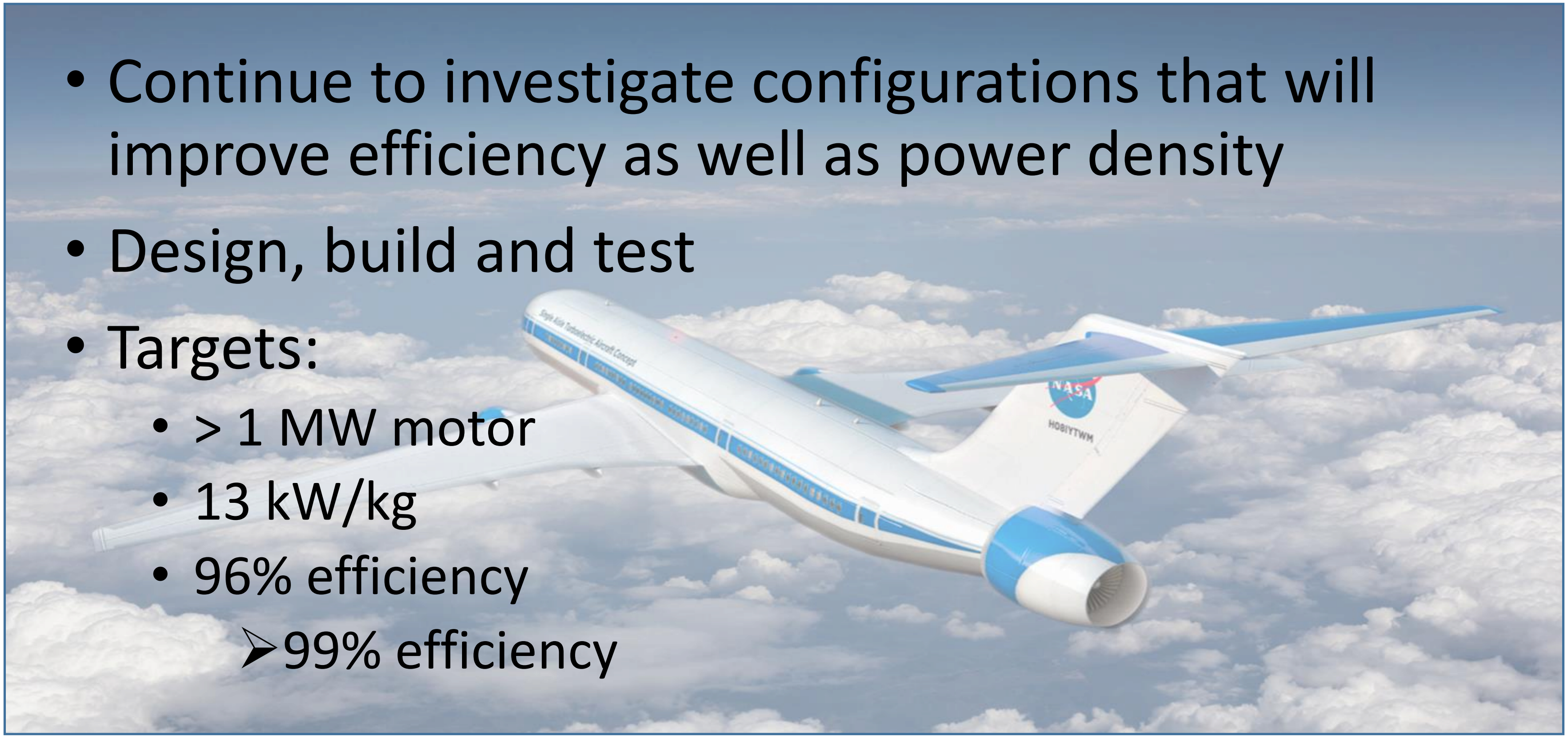

- Continue to investigate configurations that will improve efficiency as well as power density
- Design, build and test
- Targets:
  - > 1 MW motor
  - 13 kW/kg
  - 96% efficiency
    - ➢99% efficiency

Acknowledgments

This work was funded by NASA:
Advanced Air Vehicle Program
Advanced Air Transport Technology Project
Hybrid Gas-Electric Propulsion Subproject
Amy Jankovsky subproject manager

Thanks to the non-cryogenic motor team members from NASA:

- *Yaritza de Jesus-Arce – team leader*
- *Cheryl Bowman*
- *Ryan Edwards*
- *Ralph Jansen*
- *Peter Kascak*
- *Andrew Provenza*

Results – Increasing Speed

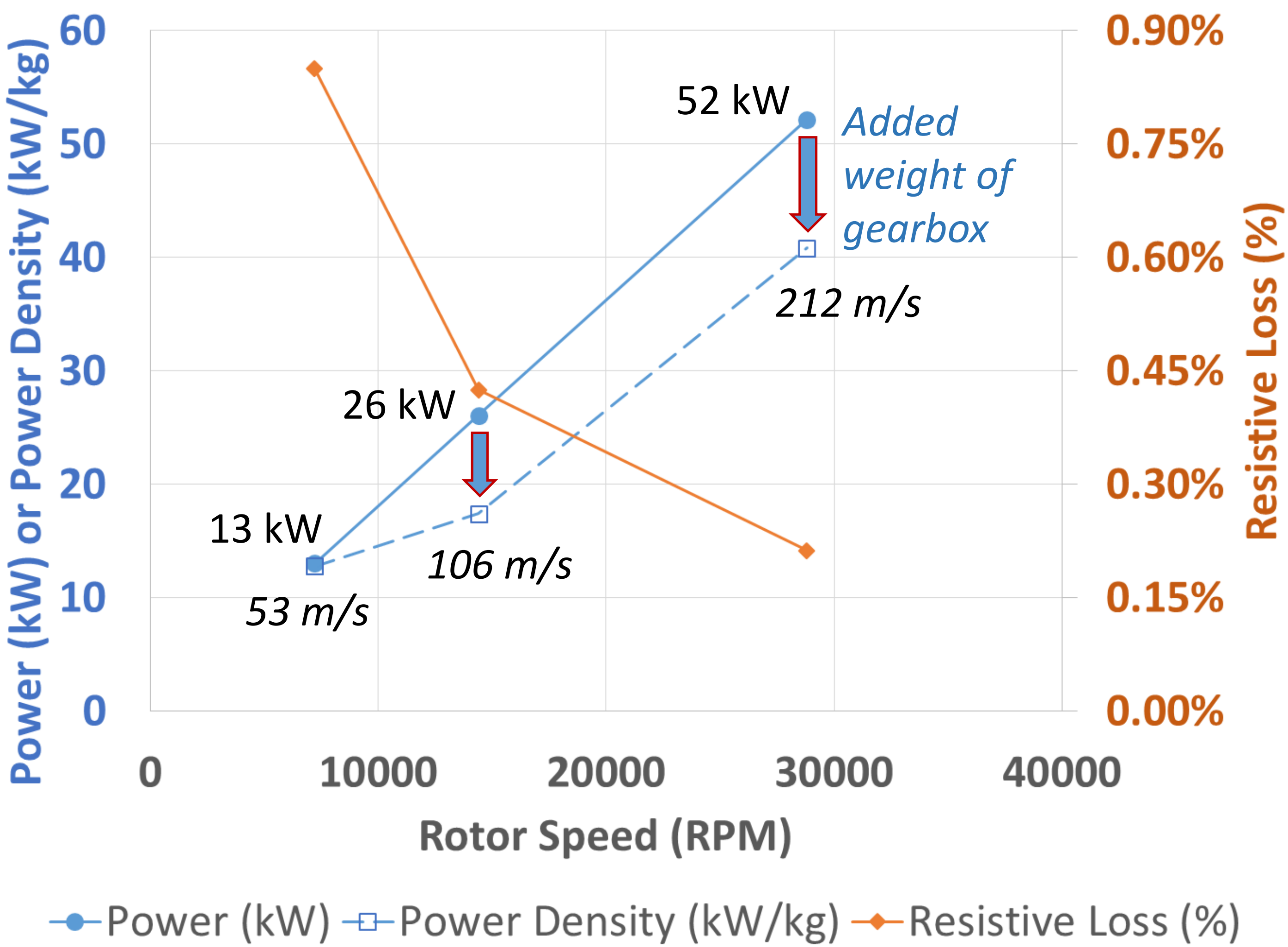

Results – Increasing Speed

Redesigned for 13 kW with Gearbox

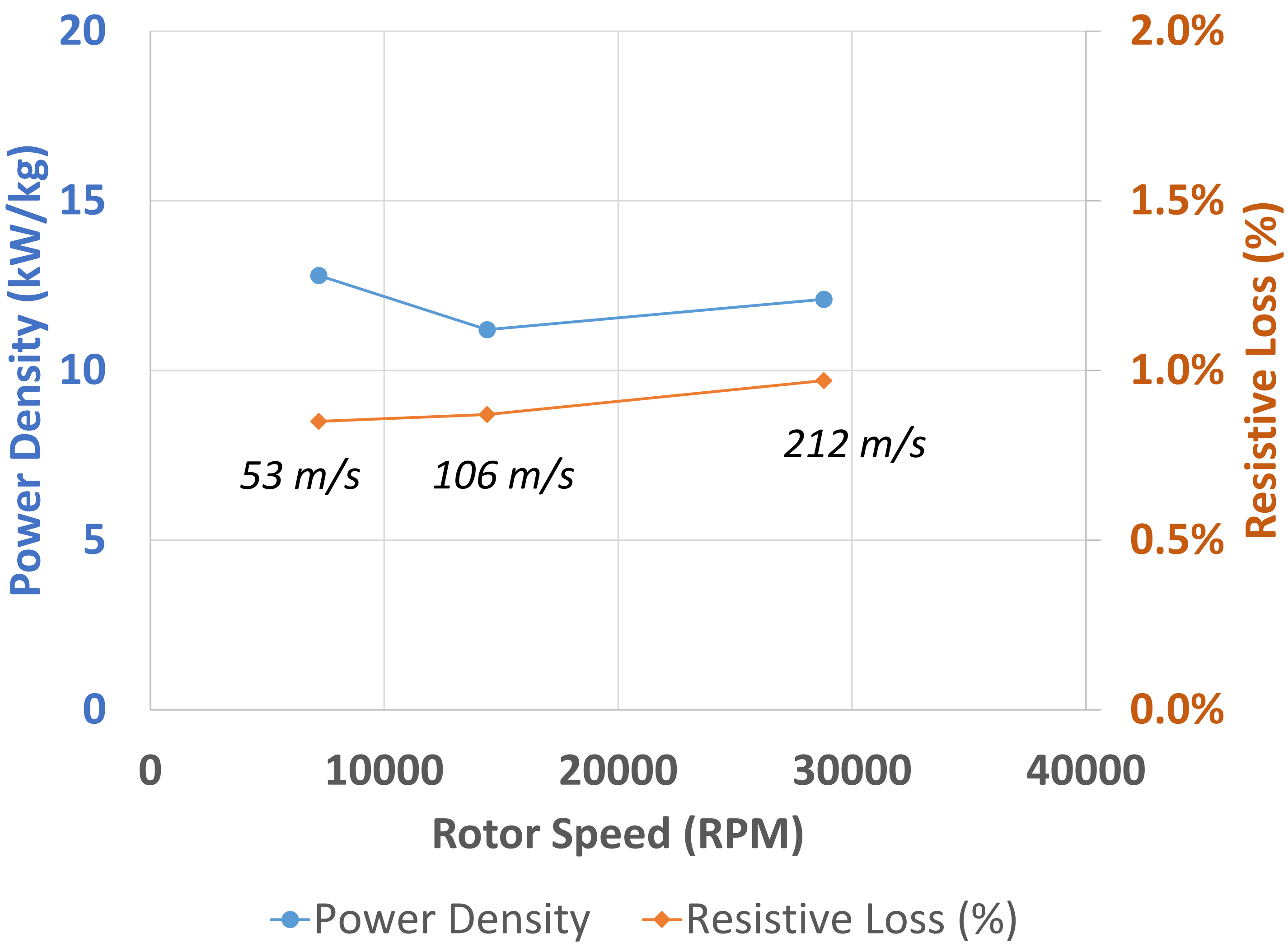

3D Transient vs 2D Static Results

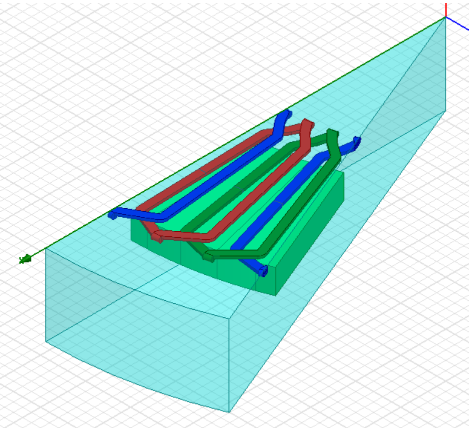

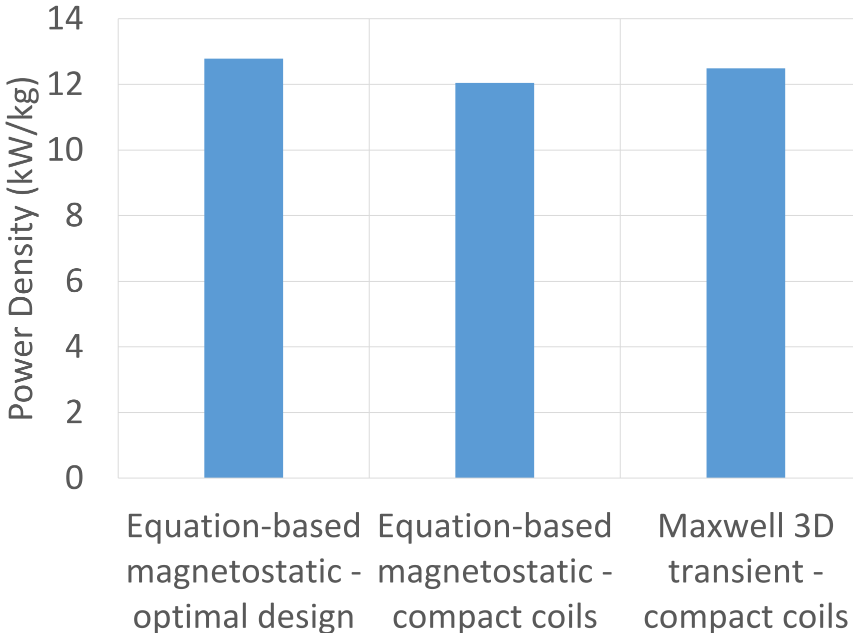

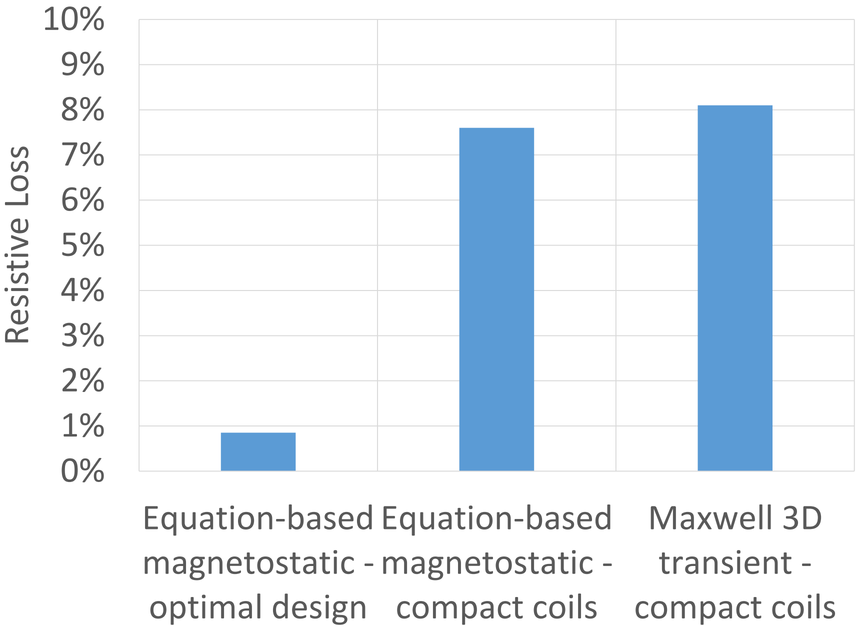

3D Transient vs 2D Static Results

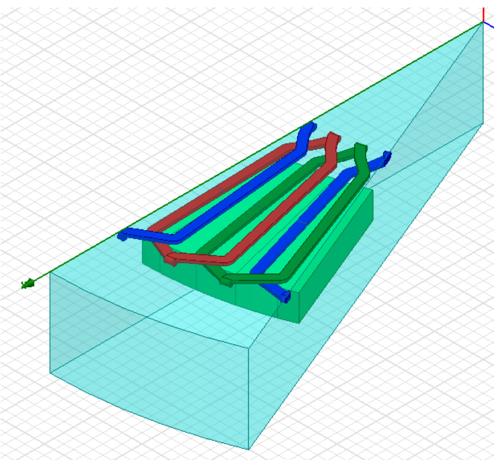

Analysis	Torque (N-m)	Resistive Loss (%)	Eddy Current Loss Conductors (%)	Eddy Current Loss Magnets (%)
Equation-based magnetostatic large coils/optimal	17.3	0.85%	0.11%	-
Equation-based magnetostatic compact coils/high J	16.3	7.6%	0.06%	-
Maxwell 3D magnetostatic compact coils/high J	16.6	-	-	-
Maxwell 3D transient compact coils/high J	16.9	8.1%	-	0.02%